ANISOTROPY OF HIGH TEMPERATURE DEFORMATION OF SINGLE CRYSTAL SUPERALLOYS - CONSTITUTIVE LAWS, MODELLING AND VALIDATION

M McLean,[1] R N Ghosh,[1,2] R V Curtis,[3] U Basu-Conlin[1] and M R Winstone[4]

[1]Department of Materials, Imperial College of Science, Technology & Medicine, Prince Consort Rd, London SW7 2BP, UK
[2]National Metallurgical Laboratory, Jamshedpur, Bihar 831007, India
[3]Guy's and St Thomas's Medical & Dental School, Guy's Hospital, London SE1 9RT, UK
[4]Materials & Structures Department, Defence Research Agency, Pyestock, Hants, GU14 0LS, UK

Abstract

A model of creep deformation in single crystal superalloys accounts for the tertiary creep behaviour through a damage parameter that is related to the accumulation of mobile dislocations and for the anisotropies and asymmetries of creep by the viscous glide on two families of slip systems. Creep curves for the single crystal superalloy SRR99 have been analysed. Among aspects of the deformation of single crystals predicted by the model and validated by experiment are the dependence of the relative creep strengths of $<100>$ and $<111>$ orientations on stress and temperature and the changes in orientation and specimen cross-section with creep strain.

Acknowledgements

The work was supported by the Defence Research Agency. UB-C receives an SERC CASE Studentship supported by European Gas Turbines Ltd.

Superalloys 1992
Edited by S.D. Antolovich, R.W. Stusrud, R.A. MacKay, D.L. Anton, T. Khan, R.D. Kissinger, D.L. Klarstrom
The Minerals, Metals & Materials Society, 1992

Introduction

The technological impact of single crystal turbine blades has been one of the most important features of superalloy development over the past decade. The critical contribution to this technology has been the identification of a range of alloy compositions specific to the single crystal form (1,2,3). Although the temperature capabilities of these materials are undoubtedly significantly higher than those of the conventionally cast and directionally solidified alternatives, it is unlikely that their full potential has yet been fully realised because of the difficulties in fully accounting for the crystallographic anisotropies in both the compilation of a database of mechanical properties and in engineering design, particularly in conditions of complex and varying stress.

The creep behaviour of single crystal superalloys has a range of characteristics that are not generally accounted for in databases of mechanical properties.

- The creep curve shows a progressive increase in creep rate over most of the specimen life. This extended tertiary creep behaviour is also exhibited by most isotropic superalloys.

- The creep behaviour is a strong function of crystal orientation in addition to being dependent on stress σ and temperature T. The relative creep strengths of different orientations vary with both stress and temperature for a given alloy and alloys differ in their levels of anisotropy (4).

- Crystal orientations, in general, vary during deformation. It is only the simple symmetrical $<100>$ and $<111>$ orientations that are stable under axial loading.

- Asymmetric deformation leads to changes in component shape causing, for example, cylindrical specimens to develop increasingly elliptical cross-sections.

A test programme to fully characterise all of these features as functions of the principal test variables, stress and temperature, for each alloy would be impracticable because of the large number of variables. Rather, it is necessary to develop a strategy to account for the observed complexities of behaviour in terms of a more limited database.

There has been considerable success in modelling the highly non-linear creep behaviour of isotropic engineering alloys including nickel-base superalloys. For example, the empirical Graham-Walles representation (eg Candler and Winstone (5)) and the θ-projection method of Evans and Wilshire (6) can represent creep curve shapes of a wide range of materials. Barbosa et al (7) described an alternative physics-based modelling approach to the analysis of superalloy creep that accounts for the dominant tertiary behaviour in terms of a range of damage mechanisms and that can be extended to account for more complex loading conditions (8).

The present study, which is an extension of the work described by Barbosa et al, develops and evaluates a physics-based model of creep in single crystals that accounts for both the tertiary creep behaviour and the anisotropic deformation that is manifested in the complex and asymmetric characteristics of single crystal superalloys outlined above. The basis of the model, which as been described by Ghosh et al (9), is that even in creep conditions plastic deformation occurs on a restricted number of slip systems; this assumption is in agreement with many detailed microstructural studies (10,11) although there is some debate over the detailed identification of the operative slip vectors. This paper will explore the implications of the model to different aspects of deformation and will compare the predictions with experimental observations and measurements.

Isotropic Model and Symmetric Orientations

The isotropic model described by Barbosa et al (7) considers the creep rate $\dot{\varepsilon}$ at any time to be determined by the current values of two state variables S and ω that are related to the evolution of microstructure of the material. S is an internal stress that progressively increases to an asymptotic

steady state value S_{ss} and leads to the initial primary creep behaviour. The damage parameter ω can have contributions from a variety of mechanisms including the change in alloy microstructure, development of grain boundary cavities and changes in specimen cross-section. For single crystals tested under constant stress conditions only the microstructural contribution need be considered.

Recent analyses, both theoretical (12) and experimental (13,14) have shown $\dot{\varepsilon}$ to be a linear function of ω rather than the exponential function described by Barbosa et al (7). The creep behaviour is described by a coupled set of differential equations that can be integrated numerically to account for the strain-time evolution:

$$\dot{\varepsilon} = \dot{\varepsilon}_i(1 - S)(1 + \omega)$$

$$\dot{S} = H\dot{\varepsilon}_i(1-S) - \frac{H\dot{\varepsilon}_i}{S_{ss}}S \qquad (1)$$

$$\dot{\omega} = C\dot{\varepsilon}$$

Any individual creep curve is fully described by the four parameter set ($\dot{\varepsilon}_i$, S_{ss}, H, C) and procedures have been developed to evaluate these parameters by analysis creep curves (7).

The isotropic model has been used to analyse a database of tensile creep curves for <001> oriented single crystals of SRR99 tested under constant stress conditions at a wide range of stresses and temperatures. For this orientation there are no significant crystal rotations and deformation is quite symmetrical. Consequently the simple model would appear to be appropriate. Each individual creep curve was analysed using the CRISPEN software developed by the National Physical Laboratory to determine the optimum values of the model parameters; Figure 1 shows a typical fit of the curve generated by Equation Set 1 to the experimental points.

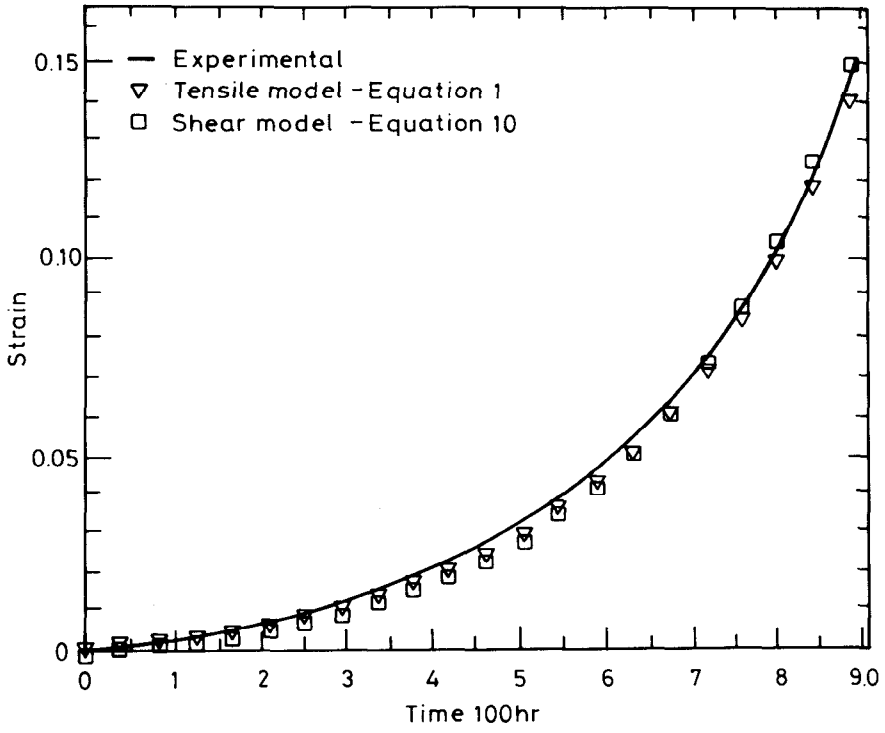

Figure 1 - Comparison of an experimentally measured creep curve with the fits of the isotropic and anisotropic model for <001> orientation of SRR99 tested at 450 MPa, 850°C

Curtis and McLean (14) have made a detailed analysis of the variations of the model parameters with stress and temperature for <001> crystals of SRR99. They can be represented by the following values and expressions for the model parameters:

$$H = 3.3 \times 10^5 \text{ MPa} \tag{2}$$

$$S_{ss} = 0.95 \tag{3}$$

$$C = \text{minimum } \{A_3 \exp(-A_4\sigma - \frac{Q_2}{RT}) \text{ or } C_o\} \tag{4}$$

$$\dot{\varepsilon}_i = A_1 \exp(A_2\sigma - \frac{Q_1}{RT}) \tag{5}$$

where A_1, A_2, A_3, A_4, Q_1 and Q_2 are constants. Thus an eight parameter set can be used to represent fully the creep behaviour over the entire range of stresses and temperature considered.

Figure 2 compares the measured times to 5% strain and to rupture with the values calculated using Equations 1-5. The agreement for rupture life is generally within the experimental scatter for temperatures below ~1000°C where there is no extensive γ' rafting. There is an additional deviation at low strains at 750°C associated with the higher levels of primary creep that occur at low temperatures. However, the model implemented on a standard IBM compatible personal computer provides a good representation of a wide range of creep curves. The differential formulation of Equation Set 1 allows creep strain under varying stresses and temperatures to be computed in a straightforward manner.

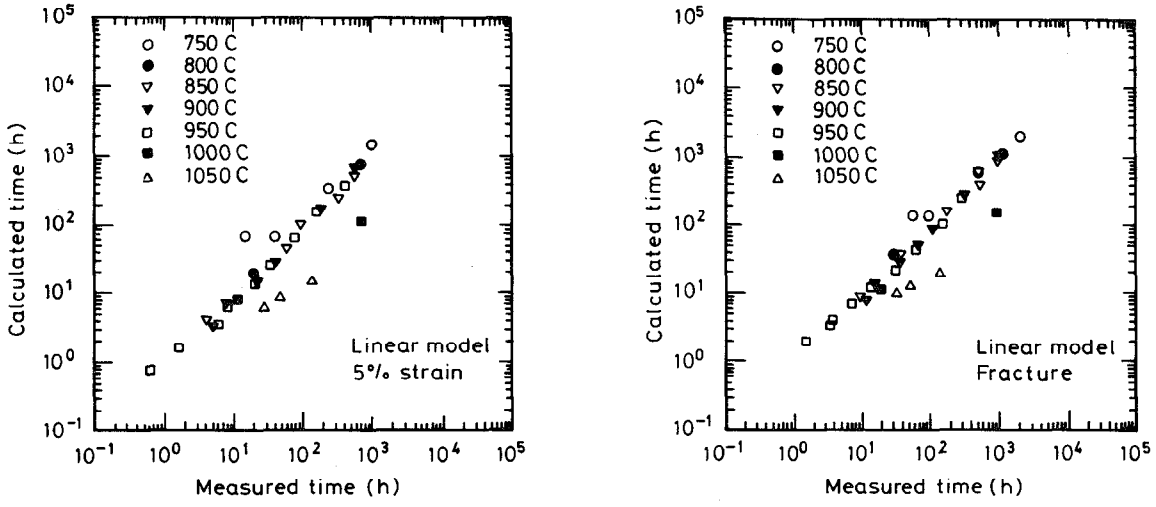

Figure 2 - Comparison of the measured times to 5% extension and rupture for a creep database of <001> oriented SRR99 with the predictions of the isotropic model.

Anisotropic Model and Data Analysis

The isotropic model is expressed in terms of tensile stresses and tensile strains. However, there is now firm evidence from detailed electron microscope studies (3,10,11) that, even in long term creep conditions, deformation in single crystal superalloys occurs by dislocations operating under local shear stresses on well defined glide systems to produce a shear strain. Ghosh et al (9) have described in some detail the formulation of a model of creep in which deformation occurs by time dependent glide in specific crystallographic directions. The model retains the characteristic of

increasing damage to represent the tertiary creep behaviour. When applied to a single crystal superalloy, Ghosh et al (9) show that it is necessary to incorporate glide on both octahedral and cube planes in order to account for the observed creep anisotropies. The model represented by Equation Set 1 can be reformulated in terms of shear creep on each allowed glide system, the tensile strain observed being the accumulation of many shear displacements.

Model formulation

The basic assumption is that all of the N possible slip systems of the allowed type, $(n_1\ n_2\ n_3)\ [b_1\ b_2\ b_3]$ say, will be active and shear at a rate dependent on the local resolved shear stress τ^k and on temperature T. The displacement vector e_{ij}, defined with respect to the cube axes can be determined by summation of the various shear components

$$e_{ij} = \sum_{k=1}^{N} \gamma^k\, b_i^k\, n_j^k \tag{6}$$

where i,j represents components along the three cubic crystal axes and have integer values of 1, 2 or 3. The summation can be extended over several types of slip systems.

In general, the small deformation represented by Equation 6 will lead to a rotation of the original tensile axis $[t_1\ t_2\ t_3]$ to a new orientation $[T_1\ T_2\ T_3]$ according to the transformation:

$$\begin{bmatrix} T_1 \\ T_2 \\ T_3 \end{bmatrix} = \begin{bmatrix} 1+e_{11} & e_{12} & e_{13} \\ e_{21} & 1+e_{22} & e_{23} \\ e_{31} & e_{32} & 1+e_{33} \end{bmatrix} \begin{bmatrix} t_1 \\ t_2 \\ t_3 \end{bmatrix} \tag{7}$$

The tensile strain ε is then simply related to the magnitude of the tensile axes before and after deformation

$$\varepsilon = \frac{\bar{T} - \bar{t}}{\bar{t}} \tag{8}$$

The asymmetry of deformation can similarly be related to the different changes in vectors in various directions in the plane normal to the original tensile axis. The initial and final transverse vectors $[x_1\ x_2\ x_3]$ and $[X_1\ X_2\ X_3]$ are related by a similar transformation as Equation 7 and the transverse strain ε_t is given by the change in magnitude of these vectors

$$\varepsilon_t = \frac{\bar{X} - \bar{x}}{\bar{x}} \tag{9}$$

In this analysis, two specific slip systems are considered to be active - viz $\{111\} <\bar{1}01>$ and $\{001\} <110>$. The rate of shear deformation on each of them is represented by a set of coupled differential equations of the form of Equation 1.

$$\begin{aligned} \dot{\gamma} &= \dot{\gamma}_i(1 - S)(1 + \omega) \\ \dot{S} &= H\dot{\gamma}_i\,(1 - S) - \frac{H\dot{\gamma}_i}{S_{ss}}\,S \\ \dot{\omega} &= \beta\dot{\gamma} \end{aligned} \tag{10}$$

Deformation on each system is represented by the four parameters ($\dot{\gamma}_i$, S_{ss}, H, β) of which $\dot{\gamma}_i$ and β have strong dependencies on shear stress and temperature represented by:

$$\dot{\gamma}_i = a_1 \exp\left(a_2\tau - \frac{Q_1}{RT}\right) \tag{11}$$

and

$$\beta = a_3 \exp\left(-a_4\tau - \frac{Q_2}{RT}\right) \tag{12}$$

The creep behaviour can be calculated numerically using Equations 6-12 using similar procedures to those used in the isotropic model with the added complexity that the orientation is redefined after each time step in the calculation.

Data analysis

As indicated above, for an arbitrary crystal orientation the model predicts that tensile strain will be accompanied by a change in orientation and a shape distortion. However, for axial loading of the simple orientations <100> and <111> the active slip systems are symmetrically oriented with respect to the axis of loading and this stabilises the material orientation and shape. For these special orientations, the tensile and shear formulations of the model are exactly equivalent there being simple geometrical relationships between the model parameters (see Ghosh et al (9) for details).

Since a <100> axial stress has zero resolved shear stress on cube planes, analysis of tensile creep data for <100> oriented crystals gives information only on $\{111\}\langle\bar{1}01\rangle$ glide. Similarly, a <111> axial stress has a much greater resolved shear stress on cube than on octahedral planes enabling the parameters for {001} <110> glide to be evaluated from <111> tensile creep data. Figure 1 shows the level of agreement in calculations using the tensile and shear formulations for a typical tensile creep curve for <100> oriented SRR99.

Constant stress creep curves at a range of stresses and temperatures for specimens of SRR99 of <100> and <111> orientations have been analysed to produce the database of 14 parameters required by the anisotropic model formulation. Available data for <100> orientations covered a more comprehensive range of stresses and temperatures than for <111>. Consequently, the evaluation of the model parameters for cube slip may be subject to some uncertainty making the predictions indicative rather of high quantitative precision.

Model Predictions and Experimental Validation

Having established the model parameter database for SRR99, Equations 6-12 are used to calculate various characteristics of the anisotropy of creep deformation that were highlighted in the introduction and to compare the calculated behaviour with experimental observations.

Relative creep performance of <100> and <111>

Creep curves for <100> and <111> orientations subject to various tensile stresses and temperatures have been calculated using the model and the database for SRR99. There is no simple relationship between the predicted creep strengths of the two orientations. The results are summarised in Figure 3 which plots the ratio of the calculated times for <100> and <111> specimens to achieve 20% strain as a function of the applied tensile stress at various temperatures. The variation in the relative creep strengths of the two orientations is due to the different stress and temperature dependencies for glide on the $\{111\}\langle\bar{1}01\rangle$ and {001} <110> systems. These predictions should be taken as indicative of the capability of the model; they are subject to considerable uncertainty because of the small <111> database.

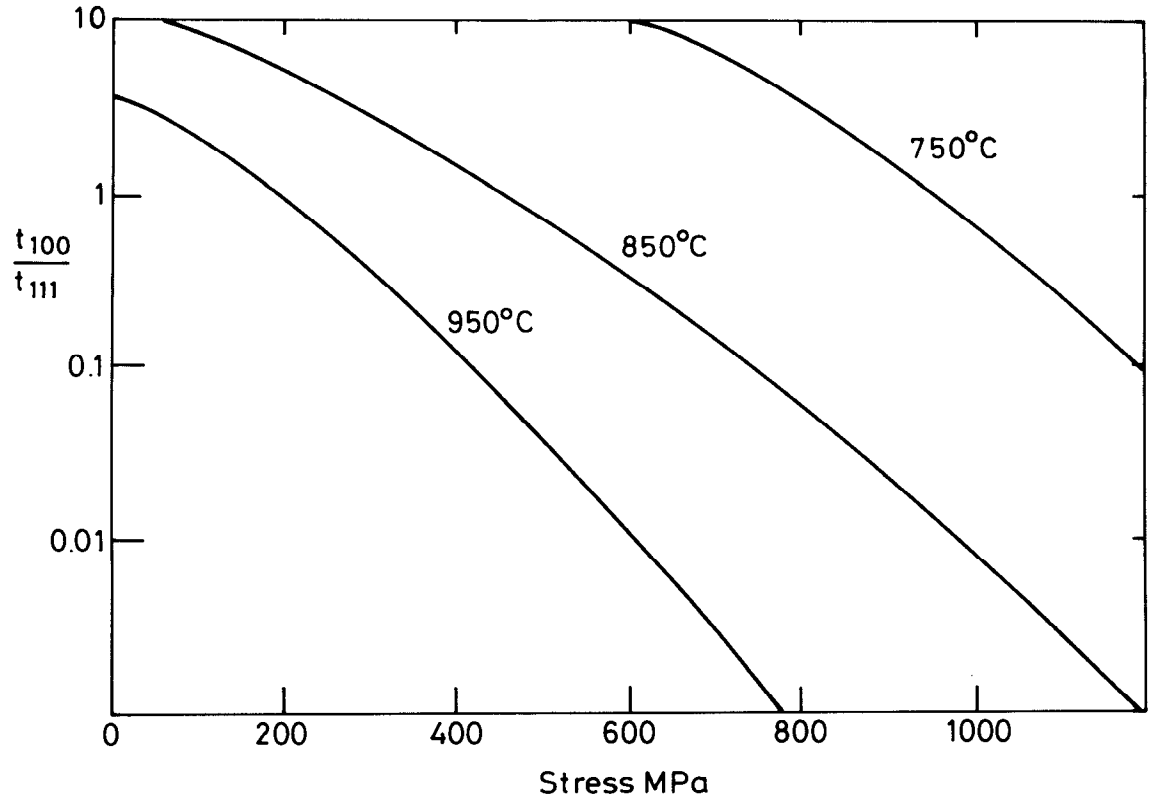

Figure 3 - Ratio of times for 20% creep strain for <001> and <111> orientations of SRR99 as a function of stress and temperature

Changes in orientation

The initial orientations of all single crystal creep specimens were determined prior to testing to an accuracy of about 1° by Laue X-ray back-reflection. High quality patterns were obtained from the as-solidified material; however, after creep testing the pattern was too diffuse to allow meaningful orientations to be determined. This behaviour is consistent with the accumulation of a relatively high dislocation density during deformation that introduces a significant dispersion of the atomic order over the volume of material that is sampled by the X-ray beam (~10^9 μm^3). Much higher resolution can be obtained by analysis of electron back scatter patterns (EBSP) obtained using a scanning electron microscope with the field emitter gun (~1 μm^3) as described by Quested et al (15). Using this technique the orientations at various distances along the gauge length of fractured test specimens were determined.

A full analysis of the results from this phase of the study will be given elsewhere (15). However, Figure 4a gives examples of the results obtained from creep specimens with different initial orientations that were tested at 850°C with a stress of 450 MPa. The fracture specimens exhibited significant necks indicating a large increase in local strain (reduction in area) as the fracture surface is approached. The main features of the orientation changes can be summarised as follows:

- in the specimen shoulder where there has been no significant plastic strain there is little scatter in a series of orientation determinations;

- as the fracture surface, and the zone of maximum plastic strain, is approached the orientation rotates but there is also an increased scatter in the orientation measurements.

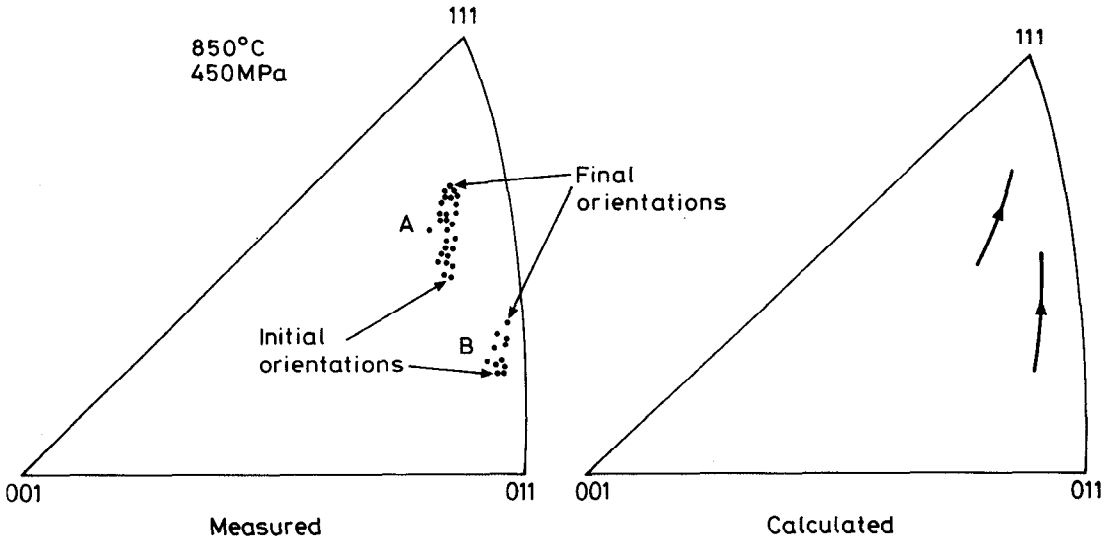

Figure 4 - Crystal rotations during creep deformation for SRR99 of different complex orientations at 850°C with a stress of 450 MPa

The model and database for SRR99 have been used to calculate the change in orientations expected for these creep conditions for the initial orientations determined. The results of the calculation that are shown in Figure 4b are generally consistent with the measurements.

Changes in specimen shape

Most specimens with complex initial orientations exhibited a significant change in specimen cross-section during creep deformation. The initially circular cross-section developed an increasingly elliptical shape as the area of cross-section was progressively reduced. The shapes of the same test specimens whose orientations were characterised above were determined as a function of the local reduction in area. A typical example of the measurements is shown in Figure 5a which plots the ratio of the maximum and minimum specimen diameters (a/b) as a function of the local reduction in area for a <234> specimen creep tested at 750°C/750 MPa. The model predictions of the changes in cross-section for these test conditions and orientation are shown in Figure 5b. The calculated ratio a/b is included in Figure 5a for comparison with the measurements.

Future developments

The model is at an early stage of development and validation. However, it is capable of extension to describe the effects of multiaxial stress states and of a wider range of loading conditions (eg strain control, stress relaxation, fatigue). The latter extension has recently been discussed by Ghosh and McLean (8) in relation to the isotropic model and will not be discussed further here. The extension to multiaxial stressing will be relatively simple for the single crystal model since no averaging criterion, such as the Van Mises stress, is used. It is only necessary to specify the resolved shear stresses on the operative slip systems resulting from the complex stress state which can be specified by three principal stresses (σ_1, σ_2, σ_3).

Figure 6 shows the calculated creep strain in the <100> direction for various multiaxial stresses at 850°C. Three different types of loading with 450 MPa along <100> are considered; the principal stress in the three cube directions are indicated. Tensile creep along <100> gives a stable orientation and material shape while shear creep gives an asymmetric deformation leading to changes in orientation and specimen shape. The model also predicts zero creep under pure hydrostatic conditions as is required by volume conservation. Further developments are required for this aspect of the model and a programme of discriminatory tests is also planned.

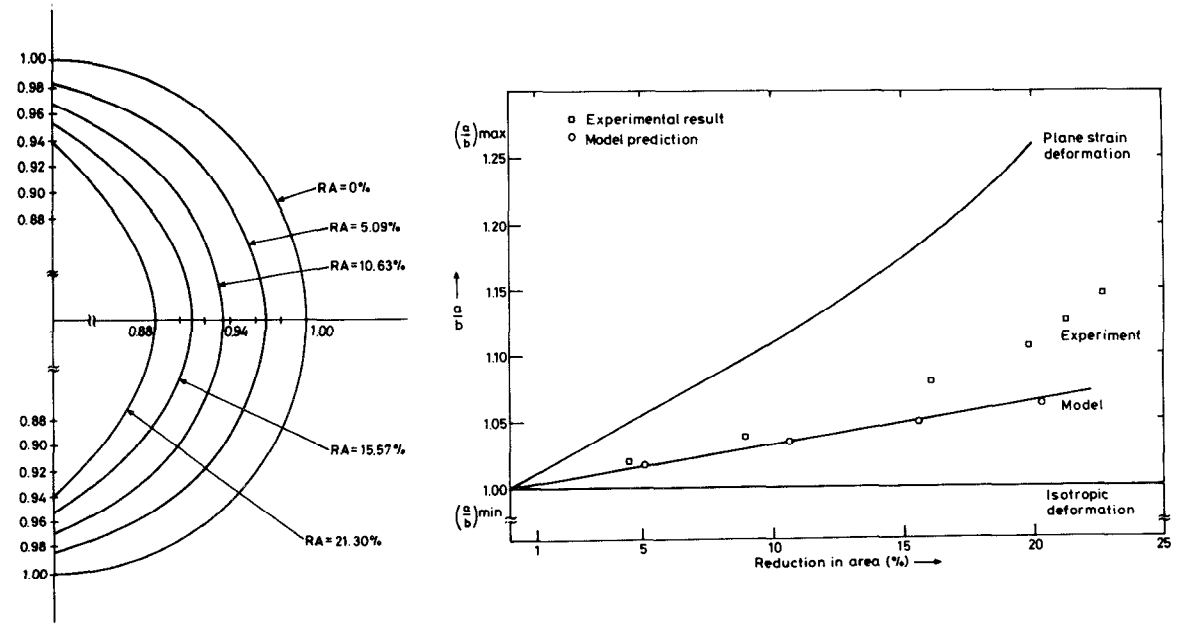

Figure 5 - (a) Calculated change in cross-sectional dimensions and shape for <234> orientation of SRR99 tested at 750°C/750 MPa, (b) Comparison of measured and calculated ratios of maximum to minimum diameter for the same test condition

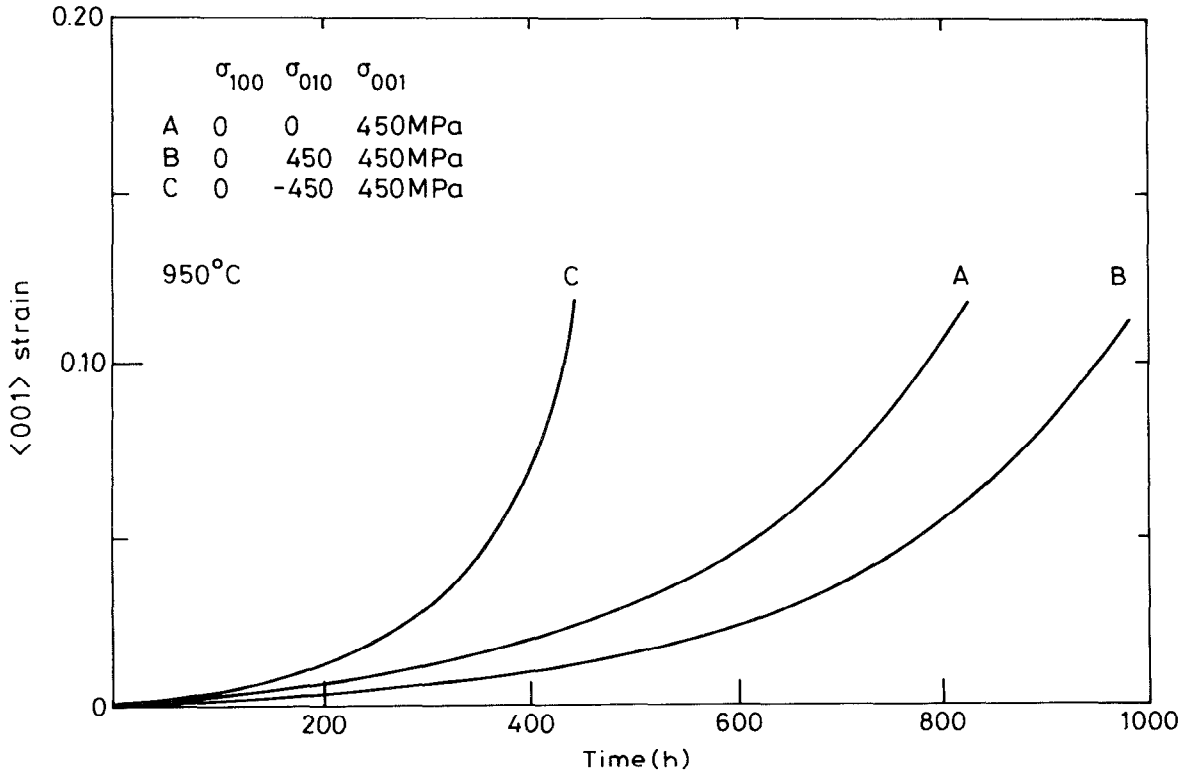

Figure 6 - Calculated creep curves for SRR99 at 950°C for different stress states indicated in the table.

Conclusions

1. A physics based model of creep deformation in single crystal superalloys has been developed that extends a previous isotropic model based on a continuum damage mechanics model.

2. The model can successfully account for several aspects of the anisotropic and asymmetric deformation of single crystal superalloys including

   - change in relative creep strength of $<100>$ and $<111>$ with stress and temperature
   - change in orientation of complex orientations with creep strain
   - change in specimen shape with creep strain for complex orientation

3. Experimental measurements of the anisotropies and asymmetries of deformation of SRR99 are largely in agreement with the model predictions.

4. The model can be extended to multiaxial stress states and other types of loading.

References

1. M Gell, A F Giamei and D N Duhl, Superalloys 1980, ed. T J Tien et al, (American Society of Metals, Metals Park, OH, 1980).

2. M J Goulette, P D Spilling and R P Arthey, Superalloys 1980, ed. G M Gell et al, (Warrendale, PA: The Metallurgical Society, 1984), 176.

3. P Caron, Y Ohta, Y G Nakagawa and T Khan, Superalloys 1988, ed. D N Duhl et al, (Warrendale, PA: The Metallurgical Society, 1988), 215.

4. M R Winstone and J E Northwood, Proc Int Conf on Metals Engineering, vol. 6, Casting and Foundry Technology, University of Aston, 15-16 September 1981.

5. L W Candler and M R Winstone, Proc of Conf on High Temperature Materials for Power Engineering, 24-27 September 1990, ed. E Bachelet et al, (Klewer Academic Publ, 1990).

6. R W Evans and G Wilshire, Materials Science and Technology, 3 (1987), 701.

7. A Barbosa, N G Taylor, M F Ashby, B F Dyson and M McLean, Superalloys 1988, ed. D N Duhl et al, (Warrendale, PA: The Metallurgical Society, 1988), 683.

8. R N Ghosh and M McLean, Acta Metall Mater, in press.

9. R N Ghosh, R V Curtis and M McLean, Acta Metall Mater, 38 (1990), 1977.

10. B H Kear and B J Piearcey, Trans Metall Soc AIME, 239 (1967), 1209.

11. Y Q Sun and P M Hazzledine, Phil Mag, A58 (1988), 603.

12. B F Dyson, Rev Phys Appl, 23 (1988), 605.

13. M Maldini and V Lupinc, Scripta Metall, 22 (1988), 1737.

14. R V Curtis and M McLean, to be published.

15. P N Quested, P J Henderson and M McLean, Acta Metall, 36 (1988), 2743.